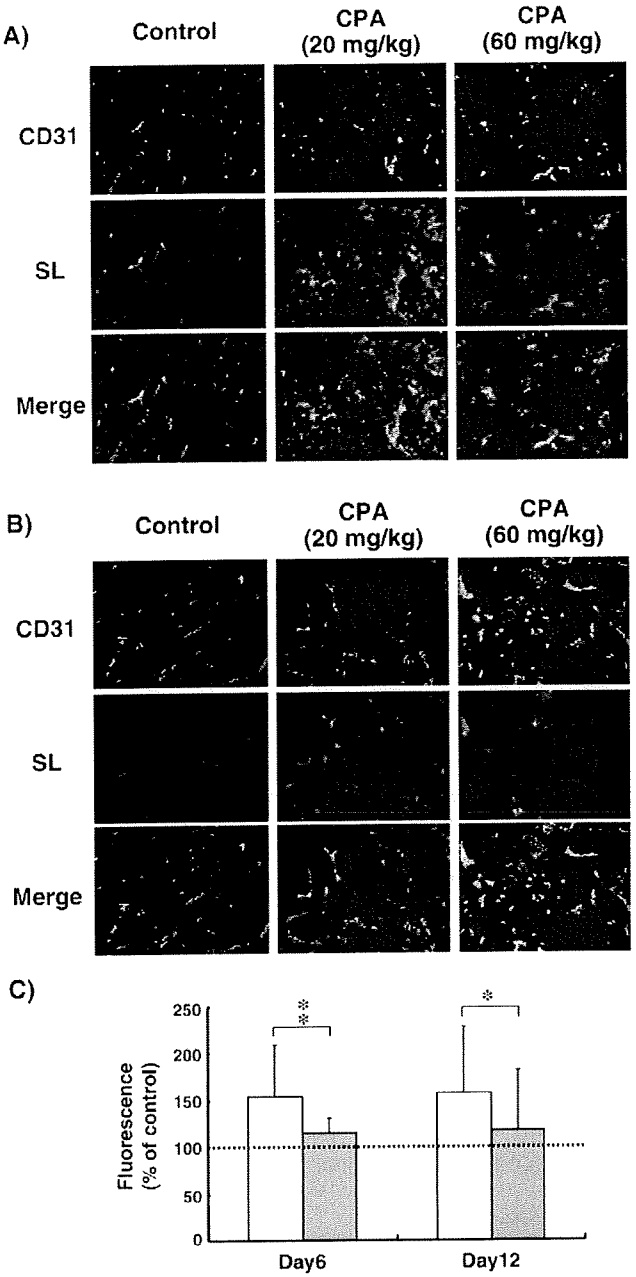

Fig. 4. Distribution of liposomes in tumor tissue. Immunofluorescence analysis of CD31$^+$ microvessels and fluorescence analysis of SL in the solid tumors (n=4–5). On day 5 (A) or day 11 (B) after tumor inoculation, CPA (20 or 60 mg/kg) was orally administered and subsequently DiI-labeled SL intravenously injected. 24 h later, cryosections of the tumor tissue were FITC-immuno-stained for the CD31$^+$ microvessels and then examined for FITC (green) and DiI (red) fluorescence. (C) Quantification of fluorescence intensity of DiI (representing SL). Open columns represent data from the tumor treated with CPA (20 mg/kg). Shaded columns represent data from the tumor treated with CPA (60 mg/kg). *, $p<0.05$; **, $p<0.01$ versus Control. Magnification, x100.

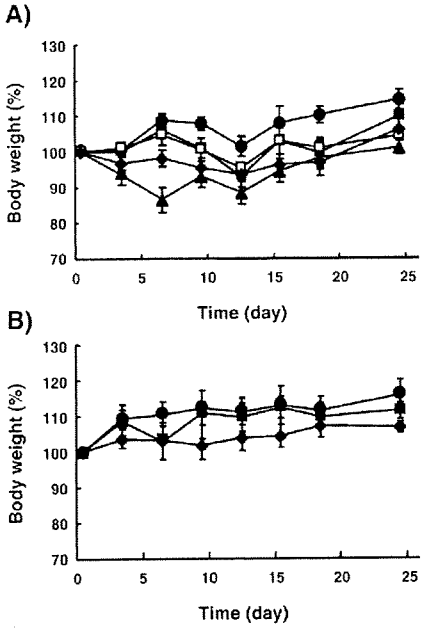

Fig. 5. Body weight change. (A) Monotherapy: Control (●), Conventional CPA dosing (MTD) (▲), CPA (20 mg/kg) at 3-day intervals (□), CPA (60 mg/kg) at 3-day intervals (■), DXR-SL (1 mg/kg) at 3-day intervals (◆). (B) Combination therapy: Control (●), CPA (20 mg/kg) and DXR-SL (1 mg/kg) at 3-day interval (■), CPA (60 mg/kg) and DXR-SL (1 mg/kg) at 3-day interval (◆). n=5 mice per group.

combination chemotherapy was estimated by measuring changes in body weight and WBC number.

A conventional CPA dosing schedule (MTD) led to a transient weight loss that was restored by the end of the cycle (Fig. 5A). As opposed to MTD of CPA, other monotherapeutic regimens did not cause weight loss but led to a mild delay in weight gain (Fig. 5A). The combination therapies did not cause any weight loss (Fig. 5B). However, the combination therapy with the higher CPA dose (60 mg/kg) led to suppression in weight gain (Fig. 5B). Tissue weights of treated mice (heart, lung, liver, kidney, and spleen) were not different from those of control mice (data not shown).

Two days after the last MTD CPA dose, WBC number was strongly reduced, followed by a strong overshoot at day 10 and restoration to normal levels by day 24 (Fig. 6A). Monotherapies also reduced the number of WBC, but the reduction was less dramatic than upon the

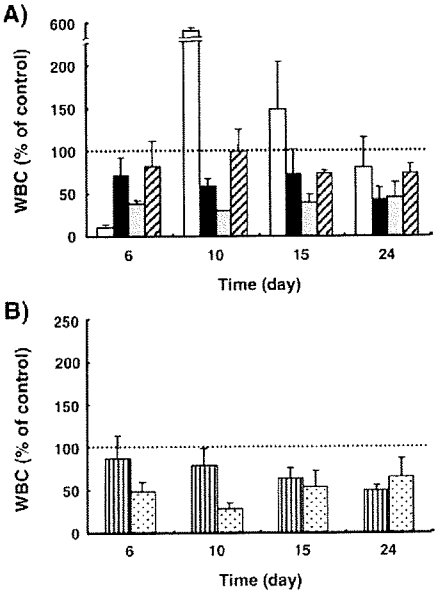

Fig. 6. Change in peripheral white blood cell (WBC) number relative to control (no treatment). (A) Monotherapy: Conventional CPA dosing (MTD) (white bars), CPA (20 mg/kg) at 3-day intervals (black bars), CPA (60 mg/kg) at 3-day intervals (grey bars), DXR-SL (1 mg/kg) at 3-day intervals (hatched bars). (B) Combination therapy: CPA (20 mg/kg) and DXR-SL (1 mg/kg) at 3-day interval (striped bars), CPA (60 mg/kg) and DXR-SL (1 mg/kg) at 3-day interval (dotted bars). n=5 mice per group.

conventional CPA dosing (MTD) (Fig. 6A). The combination regimens led to reduction in the number of WBC with no subsequent overshoot in WBC number (Fig. 6B). The reduction was similar to that observed for the metronomic CPA-dosing schedule. These findings indicate that adding DXR-SL to the metronomic CPA-dosing schedule does not increase bone marrow toxicity of CPA.

4. Discussion

The combination of a metronomic CPA dosing schedule with sequential injections of DXR-SL exerts synergistic antitumor activity in murine solid tumor model, as compared to administration of either treatment alone (Figs. 1 and 2), with no-overlapping toxic side effects (Figs. 5 and 6). It is generally accepted that long-circulating liposomes, such as sterically stabilized (PEGylated) liposomes (SL), accumulate in solid tumors via angiogenic blood vessels that have increased permeability [8] due to the so-called "EPR effect" [7]. Metronomic chemotherapy using CPA induces apoptosis in the endothelial cells of the growing tumor vasculature [6]. Therefore, we proposed that metronomic CPA dosing may increase the permeability of tumor microvessels to macromolecules during or before causing the collapse of microvessels, resulting in enhanced extravasation and subsequent accumulation of SL in the solid tumor. In this study, we confirmed that metronomic CPA dosing promotes enhanced accumulation of SL in the tumor tissue in a CPA-dose dependent manner (Fig. 4). This enhancing effect probably reflects the transient increase in density of microvessels in the tumor tissues (Fig. 3). Anti-angiogenic therapy causes tumor tissue hypoxia by diminishing blood flow, and the resulting hypoxia and acidification of the surrounding tissue can induce expression of angiogenic factors in the tumor [18]. Thus, metronomic CPA dosing might enhance subsequent angiogenesis in the tumor during drug-free intervals (for 2 days) (Fig. 3).

It is noteworthy that, in the metronomic CPA dosing, SL were found to penetrate deeply into the tissue (Fig. 4). The abnormalities in vessel and microenvironment of solid tumors may result in insufficient drug delivery and therapeutic efficacy [19]. Normalization of tumor vascular has been proposed to enhance drug delivery and improve tumor response to chemotherapy [20–22]. The metronomic CPA dosing may transiently normalize the tumor vasculature and microenvironment, because the therapy produces thrombospondin 1 (TSP1) [23] which is a well known endogenous inhibitor of angiogenesis [24]. Accompanied by vascular normalization, decreased interstitial fluid pressure would restore the pressure gradient across the blood vessel wall as well as tumor interstitium and thus, increase penetration of sequentially administered CPA in the tumor [22,25]. As a consequence, adequate CPA levels may be reached in the tumor tissue and lead to an enlargement in the tumor interstitial space into which SL is able to diffuse.

The density of $CD31^+$-microvessels in the treated tumors tended to decrease in a time after tumor-inoculation dependent manner, although the densities transiently increased in response to each CPA administration (Fig. 3). In addition, the combination chemotherapy with the *lower dose* CPA (20 mg/kg) and DXR-SL (1 mg/kg), led to a synergistic anticancer effect only when the therapy was applied in the early stage of tumor growth (day 5 after tumor inoculation) (Figs. 1 and 2). This suggests that metronomic CPA treatment-induced SL extravasation and diffusion would be transient and depend on the stage of tumor. Therefore, the timing, duration and extent of "enhanced extravasation window" towards SL are critical parameters of the metronomic CPA treatment. This strategy may extend to other types of anti-angiogenic and vasoactive agents. In fact, Kano et al. [26] recently reported that a low dose of transforming growth factor type I receptor (TβR-I) inhibitor promoted accumulation of nanocarriers (polymeric micelles) in a solid tumor. They showed that TβR-I inhibitor specifically increases the permeability of the tumor neovasculature by decreasing the degree of coverage of the endothelium without decreasing the number of endothelial cells, resulting in enhanced extravasation of the nanocarriers and an increase in therapeutic efficacy of the DXR-containing nanocarrier. In addition, ten Hagen and co-workers showed that co-administration of tumor necrosis factor-α (TNF-α) and liposomal DXR (DXR-SL) resulted in drug accumulation accompanied by pronounced tumor response in both rat and murine tumor models [27,28]. Accordingly, understanding the cellular and molecular mechanisms of the extravasation process of SL as observed in this study would be an important step towards the application and improvement of this strategy. Modification and control of the enhanced extravasation process may exhibit further synergistic effects by combination of liposomal anticancer agents and anti-angiogenic treatment.

We recently reported that the combination of a metronomic CPA dosing schedule with sequential injections of DXR-SL increases therapeutic efficacy in the murine lung metastatic B16BL6 melanoma model [15]. Under some dosage regimens, the therapeutic efficacy was accompanied by an increase in toxic side effects [15]. Therefore, we now improve the CPA regimen, i.e. reduction in each dose and total dose, and changing the dosage route. In addition, the dose of DXR-SL was set at 1 mg/kg, which was the low dose in our previous study [15]. Consequently, no overlapping toxic side effects were observed (Figs. 5 and 6). Originally, metronomic chemotherapy with CPA shows lower toxicity, because the dosage regimen refers to the frequent administration of CPA at relatively low, minimally toxic dose [1,6]. DXR is used to treat patients with sarcoma, lymphoma, and breast and ovarian carcinoma [29]. But its use is limited by potential cardiac toxicity, particularly at cumulative doses greater than 400 mg/m^2 [29]. Encapsulation of DXR in SL lowered its toxicity [12,13]. On the other hand, it has been reported that DXR-SL causes secondary cumulative adverse events in the later treatment cycle, namely stomatitis and skin-toxicity [12,30–33]. The novel dosage regimen, i.e. the metronomic CPA dosing plus DXR-SL, may overcome the limitations of DXR-SL, resulting in prolongation of survival and improvement on quality of life in patients. CPA and DXR-SL already have been approved for clinical use. Therefore, the combined regimen (metronomic CPA dosing plus DXR-SL) is considered to hold promise for approval in clinical use.

In conclusion, we show that metronomic CPA dosing augmented the accumulation of SL in a solid tumor by increasing the density of microvessels, which may have enhanced permeability towards 100-nm SL. This strongly correlated with an increased anti-tumor response. Because both CPA and DXR-SL (Doxil) are approved for clinical use, this regimen is considered to hold promise of clinical benefit in the treatment of intractable solid tumors.

Acknowledgements

We thank Dr. G.L. Scherphof for his helpful advice in writing the English manuscript. This study was supported in part by the Kobayashi Fund for Cancer Research and the Knowledge Cluster Initiative from Ministry of Education, Science and Technology.

References

[1] R.S. Kerbel, B.A. Kamen, The anti-angiogenic basis of metronomic chemotherapy, Nat. Rev. Cancer 4 (2004) 423–436.
[2] J. Gille, K. Spieth, R. Kaufmann, Metronomic low-dose chemotherapy as antiangiogenic therapeutic strategy for cancer, J. Dtsch. Dermatol. Ges. 3 (2005) 26–32.
[3] B. Laquente, F. Vinals, J.R. Germa, Metronomic chemotherapy: an antiangiogenic scheduling, Clin. Transl. Oncol. 9 (2007) 93–98.
[4] R. Munoz, S. Man, Y. Shaked, C.R. Lee, J. Wong, G. Francia, R.S. Kerbel, Highly efficacious nontoxic preclinical treatment for advanced metastatic breast cancer using combination oral UFT-cyclophosphamide metronomic chemotherapy, Cancer Res. 66 (2006) 3386–3391.
[5] Y. Shaked, U. Emmenegger, G. Francia, L. Chen, C.R. Lee, S. Man, A. Paraghamian, Y. Ben-David, R.S. Kerbel, Low-dose metronomic combined with intermittent bolus-dose cyclophosphamide is an effective long-term chemotherapy treatment strategy, Cancer Res. 65 (2005) 7045–7051.

[6] T. Browder, C.E. Butterfield, B.M. Kraling, B. Shi, B. Marshall, M.S. O'Reilly, J. Folkman, Antiangiogenic scheduling of chemotherapy improves efficacy against experimental drug-resistant cancer, Cancer Res. 60 (2000) 1878–1886.
[7] H. Maeda, J. Wu, T. Sawa, Y. Matsumura, K. Hori, Tumor vascular permeability and the EPR effect in macromolecular therapeutics: a review, J. Control. Release 65 (2000) 271–284.
[8] R.K. Jain, Delivery of molecular and cellular medicine to solid tumors, Adv. Drug Deliv. Rev. 46 (2001) 149–168.
[9] D. Papahadjopoulos, T.M. Allen, A. Gabizon, E. Mayhew, K. Matthay, S.K. Huang, K.D. Lee, M.C. Woodle, D.D. Lasic, C. Redemann, F.J. Martin, Sterically stabilized liposomes: improvements in pharmacokinetics and antitumor therapeutic efficacy, Proc. Natl. Acad. Sci. U. S. A. 88 (1991) 11460–11464.
[10] A. Gabizon, R. Catane, B. Uziely, B. Kaufman, T. Safra, R. Cohen, F. Martin, A. Huang, Y. Barenholz, Prolonged circulation time and enhanced accumulation in malignant exudates of doxorubicin encapsulated in polyethylene-glycol coated liposomes, Cancer Res. 54 (1994) 987–992.
[11] J. Vaage, D. Donovan, E. Mayhew, R. Abra, A. Huang, Therapy of human ovarian carcinoma xenografts using doxorubicin encapsulated in sterically stabilized liposomes, Cancer 72 (1993) 3671–3675.
[12] S.E. Krown, D.W. Northfelt, D. Osoba, J.S. Stewart, Use of liposomal anthracyclines in Kaposi's sarcoma, Semin. Oncol. 31 (2004) 36–52.
[13] T. Safra, F. Muggia, S. Jeffers, D.D. Tsao-Wei, S. Groshen, O. Lyass, R. Henderson, G. Berry, A. Gabizon, Pegylated liposomal doxorubicin (doxil): reduced clinical cardiotoxicity in patients reaching or exceeding cumulative doses of 500 mg/m^2, Ann. Oncol. 11 (2000) 1029–1033.
[14] T. Ishida, R. Maeda, M. Ichihara, K. Irimura, H. Kiwada, Accelerated clearance of PEGylated liposomes in rats after repeated injections, J. Control. Release 88 (2003) 35–42.
[15] E. Shiraga, J.M. Barichello, T. Ishida, H. Kiwada, A metronomic schedule of cyclophosphamide combined with PEGylated liposomal doxorubicin has a highly antitumor effect in an experimental pulmonary metastatic mouse model, Int. J. Pharm. 353 (2008) 65–73.
[16] G.R. Bartlett, Colorimetric assay methods for free and phosphorylated glyceric acids, J. Biol. Chem. 234 (1959) 469–471.
[17] E.M. Bolotin, R. Cohen, L.K. Bar, S.N. Emanuel, D.D. Lasic, Y. Barenholz, Ammonium sulphate gradients for efficient and stable remote loading of amphipathic weak bases into liposomes and ligandosomes, J. Liposome. Res. 4 (1994) 455–479.
[18] D. Fukumura, Role of microenvironment on gene expression, angiogenesis and microvascular functions in tumors. in: G.G. Meadows (Ed.), Integration/Interaction of Oncologic Growth, Springer Science+Business Media B.V, Dordrecht, 2005, pp. 23–36.
[19] R.K. Jain, Normalization of tumor vasculature: an emerging concept in antiangiogenic therapy, Science 307 (2005) 58–62.
[20] F. Winkler, S.V. Kozin, R.T. Tong, S.S. Chae, M.F. Booth, I. Garkavtsev, L. Xu, D.J. Hicklin, D. Fukumura, E. di Tomaso, L.L. Munn, R.K. Jain, Kinetics of vascular normalization by VEGFR2 blockade governs brain tumor response to radiation: role of oxygenation, angiopoietin-1, and matrix metalloproteinases, Cancer Cell. 6 (2004) 553–563.
[21] D. Fukumura, R.K. Jain, Tumor microvasculature and microenvironment: targets for anti-angiogenesis and normalization, Microvasc. Res. 74 (2007) 72–84.
[22] R.K. Jain, R.T. Tong, L.L. Munn, Effect of vascular normalization by antiangiogenic therapy on interstitial hypertension, peritumor edema, and lymphatic metastasis: insights from a mathematical model, Cancer Res. 67 (2007) 2729–2735.
[23] Y. Hamano, H. Sugimoto, M.A. Soubasakos, M. Kieran, B.R. Olsen, J. Lawler, A. Sudhakar, R. Kalluri, Thrombospondin-1 associated with tumor microenvironment contributes to low-dose cyclophosphamide-mediated endothelial cell apoptosis and tumor growth suppression, Cancer Res. 64 (2004) 1570–1574.
[24] J. Lawler, Thrombospondin-1 as an endogenous inhibitor of angiogenesis and tumor growth, J. Cell. Mol. Med. 6 (2002) 1–12.
[25] R.T. Tong, Y. Boucher, S.V. Kozin, F. Winkler, D.J. Hicklin, R.K. Jain, Vascular normalization by vascular endothelial growth factor receptor 2 blockade induces a pressure gradient across the vasculature and improves drug penetration in tumors, Cancer Res. 64 (2004) 3731–3736.
[26] M.R. Kano, Y. Bae, C. Iwata, Y. Morishita, M. Yashiro, M. Oka, T. Fujii, A. Komuro, K. Kiyono, M. Kaminishi, K. Hirakawa, Y. Ouchi, N. Nishiyama, K. Kataoka, K. Miyazono, Improvement of cancer-targeting therapy, using nanocarriers for intractable solid tumors by inhibition of TGF-beta signaling, Proc. Natl. Acad. Sci. U. S. A. 104 (2007) 3460–3465.
[27] T.L. Ten Hagen, A.H. Van Der Veen, P.T. Nooijen, S.T. Van Tiel, A.L. Seynhaeve, A.M. Eggermont, Low-dose tumor necrosis factor-alpha augments antitumor activity of stealth liposomal doxorubicin (DOXIL) in soft tissue sarcoma-bearing rats, Int. J. Cancer 87 (2000) 829–837.
[28] A.L. Seynhaeve, S. Hoving, D. Schipper, C.E. Vermeulen, G. de Wiel-Ambagtsheer, S.T. van Tiel, A.M. Eggermont, T.L. Ten Hagen, Tumor necrosis factor alpha mediates homogeneous distribution of liposomes in murine melanoma that contributes to a better tumor response, Cancer Res. 67 (2007) 9455–9462.
[29] P.K. Singal, N. Iliskovic, Doxorubicin-induced cardiomyopathy, N. Engl. J. Med. 339 (1998) 900–905.
[30] B. Uziely, S. Jeffers, R. Isacson, K. Kutsch, D. Wei-Tsao, Z. Yehoshua, E. Libson, F.M. Muggia, A. Gabizon, Liposomal doxorubicin: antitumor activity and unique toxicities during two complementary phase I studies, J. Clin. Oncol. 13 (1995) 1777–1785.
[31] F.D. Goebel, D. Goldstein, M. Goos, H. Jablonowski, J.S. Stewart, Efficacy and safety of Stealth liposomal doxorubicin in AIDS-related Kaposi's sarcoma. The International SL-DOX Study Group, Br. J. Cancer 73 (1996) 989–994.
[32] D.W. Northfelt, F.J. Martin, P. Working, P.A. Volberding, J. Russell, M. Newman, M.A. Amantea, L.D. Kaplan, Doxorubicin encapsulated in liposomes containing surface-bound polyethylene glycol: pharmacokinetics, tumor localization, and safety in patients with AIDS-related Kaposi's sarcoma, J. Clin. Pharmacol. 36 (1996) 55–63.
[33] M.I. Koukourakis, S. Koukouraki, A. Giatromanolaki, S.C. Archimandritis, J. Skarlatos, K. Beroukas, J.G. Bizakis, G. Retalis, N. Karkavitsas, E.S. Helidonis, Liposomal doxorubicin and conventionally fractionated radiotherapy in the treatment of locally advanced non-small-cell lung cancer and head and neck cancer, J. Clin. Oncol. 17 (1999) 3512–3521.
[34] A.J. Quesada, T. Nelius, R. Yap, T.A. Zaichuk, A. Alfranca, S. Filleur, O.V. Volpert, J.M. Redondo, In vivo upregulation of CD95 and CD95L causes synergistic inhibition of angiogenesis by TSP1 peptide and metronomic doxorubicin treatment, Cell. Death Differ. 12 (2005) 649–658.

Journal of Controlled Release 134 (2009) 18–25

Contents lists available at ScienceDirect

Journal of Controlled Release

journal homepage: www.elsevier.com/locate/jconrel

Oxaliplatin targeting to angiogenic vessels by PEGylated cationic liposomes suppresses the angiogenesis in a dorsal air sac mouse model

Amr Abu-Lila, Takuya Suzuki, Yusuke Doi, Tatsuhiro Ishida *, Hiroshi Kiwada

Department of Pharmacokinetics and Biopharmaceutics, Subdivision of Biopharmaceutical Sciences, Institute of Health Biosciences, The University of Tokushima, 1-78-1, Sho-machi, Tokushima 770-8505, Japan

ARTICLE INFO

Article history:
Received 24 June 2008
Accepted 23 October 2008
Available online 5 November 2008

Keywords:
Anti-angiogenic therapy
Anticancer drugs
Oxaliplatin
Cationic liposome
Dorsal air sac (DAS) model

ABSTRACT

Oxaliplatin (trans-l-diaminocyclohexane oxalatoplatinum, l-OHP) is a third-generation platinum analogue with proven anti-tumor activity against many tumor cell lines, however it does not show sufficient anti-tumor activity *in vivo* when used alone. In order to overcome this problem and to achieve an anti-angiogenic therapy with l-OHP, the drug was encapsulated into PEG-coated cationic liposomes, which were designed to target the newly formed vessels, and its anti-angiogenic activity was evaluated in an *in vivo* mouse dorsal air sac (DAS) assay. For the DAS assay, chambers filled with tumor cells were implanted underneath the dorsal skin. l-OHP encapsulated in PEG-coated cationic liposomes (5 mg/kg mice) was intravenously injected once on day 1, 2, 3 or 4 after chamber implantation. On the fifth day after chamber implantation, animals were sacrificed and tumor-angiogenesis was evaluated. Liposome-encapsulated l-OHP completely suppressed angiogenesis in the skin when it was administered day 3 after chamber implantation. Under similar experimental conditions, neither l-OHP encapsulated in PEG-coated neutral liposomes, nor free l-OHP, nor "empty" (no drug containing) PEG-coated cationic liposomes showed such strong suppressive effect. The present study suggests that the liposomal formulation of l-OHP, which targeted to angiogenic vessels, has a remarkable *in vivo* anti-angiogenic activity and the formulation may become a promising novel approach to achieve anti-angiogenic therapy.

1. Introduction

Oxaliplatin (l-OHP), a cisplatin derivative, is currently approved and marketed for second-line treatment of colorectal cancer [1,2]. It contains a bulky carrier ligand within its structure, and forms DNA adducts that more effectively inhibit DNA synthesis but are also generally considered to be more cytotoxic than adducts of either cisplatin or carboplatin [3,4]. Moreover, unlike cisplatin, it can inhibit RNA synthesis [5]. However, it has been reported that l-OHP showed a low anti-tumor activity *in vivo* when used alone [6,7]. This lower anti-tumor activity can be attributed to the high partitioning to erythrocytes and low accumulation in tumor tissues following intravenous administration. Therefore, there is an obvious need for the development of an effective way to overcome this problem. Liposomes were one of the first nanomolecular drug delivery systems to show increased delivery of small molecular weight anticancer drugs to solid tumors by altering the biodistribution of associated drugs [8,9].

Tumor angiogenesis is an essential mechanism for the adequate supply of nutrients, oxygen, growth factors and other substances to tumor cells [10–12]. Tumor angiogenesis is not a singular process; at least two types of angiogenesis are believed to contribute to vessel growth in tumors [13]. One process involves the stimulation of new blood vessel capillaries to sprout in the neighboring mature host vasculature [14,15], while the other involves the recruitment of circulating endothelial precursor cells from the bone marrow to promote neo-vascularization [16–19]. Tumor angiogenesis is mainly triggered by growth factors in the microenvironment such as vascular endothelial growth factor, (VEGF), basic fibroblast growth factor (bFGF) and the matrix metalloproteinases (MMPs) [20–22]. These factors are generally produced by the tumors themselves, by the surrounding tissue, or by infiltrating macrophages. Suppression of the angiogenesis process, leading to eradication of primary tumor cells and suppression of metastasis through the disruption of the metastatic pathway, became a promising strategy for treating solid tumors (anti-angiogenic therapy) [23–25].

To target cancer cells, nanomolecular drug delivery system including anticancer agents must first cross the vasculature and then travel through the interstitium. However, the delivery system, if targeted to tumor angiogenic vessels, has the advantage that, once in the blood stream, it should have direct access to the target endothelial

Abbreviations: bFGF, basic fibroblast growth factor; CHOL, cholesterol; DAS, dorsal air sac; DC-6-14, O,O'-ditetradecanoyl-N-(alpha-trimethyl ammonio acetyl) diethanolamine chloride; DiI, 1,1'-dioctadecyl-3,3,3',3'-tetramethylindocarbocyanine perchlorate; DMEM, Dulbecco's modified Eagle's medium; ECs, endothelial cells; FBS, fetal bovine serum; HSPC, hydrogenated soya phosphatidylcholine; l-OHP, oxaliplatin; mPEG2000-DSPE, 1,2-distearoyl-sn-glycero-3-phosphoethanolamine-n-[methoxy (polyethyleneglycol)-2000]; MMPs, matrix metalloproteinases; VEGF, vascular endothelial growth factor.

* Corresponding author. Tel./fax: +81 88 633 7260.
E-mail address: ishida@ph.tokushima-u.ac.jp (T. Ishida).

0168-3659/$ – see front matter © 2008 Elsevier B.V. All rights reserved.
doi:10.1016/j.jconrel.2008.10.018

cells in the solid tumors. It has been shown that cationic liposomes have a propensity for localizing in tumor vessels [13,26,27]. A recent study indicated that PEG-coated cationic liposomes associate with approximately 27 and 5% of vessel areas in tumors and normal tissues, respectively, in human and murine tumor models [28]. This property of selective targeting of cationic liposomes to tumor angiogenic vessels may promote the selective delivery of l-OHP to tumor endothelial cells and thus the development of chemotherapeutic strategies involving vascular targeting.

In this study we propose that the selective delivery of l-OHP to angiogenic vessels should improve its low anti-tumor activity, and more specifically achieve effective anti-angiogenic therapy. We here report the development of l-OHP-containing PEG-coated cationic liposomes and their accumulation in angiogenic vessels in a mouse dorsal air sac (DAS) model [29,30]. Finally, we investigated the anti-angiogenic effect of the preparation by using a mouse DAS model.

2. Materials and methods

2.1. Materials

Hydrogenated soya phosphatidylcholine (HSPC) and 1,2-distearoyl-sn-glycero-3-phosphoethanolamine-*n*-[methoxy (polyethyleneglycol)-2000] (mPEG$_{2000}$-DSPE) were generously donated by Nippon Oil and Fat (Tokyo, Japan). Oxaliplatin (l-OHP) was generously donated by Taiho Pharmaceutical Co. (Tokyo, Japan). Cholesterol (CHOL) and O,O'-ditetradecanoyl-N-(alpha-trimethyl ammonio acetyl) diethanolamine chloride (DC-6-14) were purchased from Wako Pure Chemical Co. Ltd (Osaka, Japan). 1,1'-dioctadecyl-3,3,3',3'-tetramethylindocarbocyanine perchlorate (DiI) was purchased from Invitrogen (OR, USA). All other reagents were of analytical grade.

2.2. Animals and tumor cell line

Male ddY mice, 5 weeks old, were purchased from Japan SLC (Shizuoka, Japan). The experimental animals were allowed free access to water and mouse chow, and were housed under controlled environmental conditions (constant temperature, humidity, and 12 h dark–light cycle). All animal experiments were evaluated and approved by the Animal and Ethics Review Committee of the University of Tokushima. The mouse melanoma cell line, B16BL6, was maintained in Dulbecco's modified Eagle's medium (DMEM) (Nissui Pharmaceutical Co. Ltd., Tokyo) supplemented with 10% heat-inactivated FBS (Japan Bioserum, Hiroshima, Japan), 10 mM L-glutamine, 100 units/ml penicillin and 100 μg/ml streptomycin in a 5% CO_2 air incubator at 37 °C. B16BL6 cell line was purchased from Cell Resource Center for Biomedical Research (Institute of Development, Aging and Cancer, Tohoku University).

2.3. Preparation of liposomes

Cationic liposomes modified with mPEG$_{2000}$-DSPE were composed of HSPC/CHOL/DC-6-14/mPEG$_{2000}$-DSPE (2/1/0.2/0.2 molar ratio). Neutral liposomes modified with mPEG$_{2000}$-DSPE were composed of HSPC/CHOL/mPEG$_{2000}$-DSPE (2/1/0.2 molar ratio). In the targeting experiments, 1 mol% of the fluorescent lipid membrane marker, DiI, was added to the lipid mixture. All liposomes were prepared using the reverse-phase evaporation method. Briefly, lipids (50 mmole) were dissolved in 6 ml of chloroform/diethyl ether (1:2 v/v) and then 2 ml of l-OHP solution (8 mg/ml) in 5% (w/v) dextrose was dropped into the lipid mixture to form w/o emulsion. For preparation of "empty" (no drug-containing) PEG-coated cationic liposomes, 5% dextrose solution was added instead of l-OHP solution. The volume ratio of the aqueous to the organic phase was maintained at 1:3. The emulsion was sonicated for 15 min and then the organic phase was removed to form liposomes by evaporation in a rotary evaporator at 40 °C under vacuum at 250 hPa for 1 h. The resulting liposomes were extruded through a polycarbonate membrane (200 nm pore size) using an extruder device (Lipex Biomembranes Inc., Canada) maintained at 65 °C to obtain liposomes of approximately 250 nm (homogeneous size). The phospholipid concentration was determined by a colorimetric assay [31]. Un-encapsulated free l-OHP was removed by dialyzing the resulting liposomes against 5% dextrose using a dialysis cassette (Slyde-A-Lyzer, 10000MWCO, PIERCE, Rockford, IL, USA). Encapsulated l-OHP was quantified using an atomic absorption photometer (Z-5700, Hitachi, Tokyo). The size and zeta potential of the liposomes were determined by using a NICOMP 370 HPL submicron particle analyzer (Particle Sizing System, CA, USA). Encapsulation efficiency of l-OHP was calculated by dividing the drug to lipid ratio after the dialysis by the initial drug to lipids ratio. Liposome suspensions were stored in glass vials at 4 °C for 4 weeks to assess their physical stabilities with respect to change in the size distribution. For the treatment with animal model, l-OHP formulations freshly prepared were used.

2.4. In vitro stability assay

l-OHP-containing liposomes (5 mmole lipids) were mixed with either 50% mouse plasma or 5% dextrose solution at a ratio of 1:9 (v/v). The l-OHP concentration in the mixture was 0.203 mg/ml for neutral liposome and 0.176 mg/ml for cationic liposome, respectively. The resulting suspension was incubated at either 37 or 4 °C. Aliquots (300–500 μl) were withdrawn at specified time points for the determination of l-OHP retention in the liposome. The l-OHP-containing liposomes were separated from the leaked drug by means of a Sepharose CL-4B column, which had been equilibrated with HEPES buffered saline (25 mM HEPES, 140 mM NaCl, pH 7.4). The amount of phospholipids and l-OHP in the liposome fractions were determined as described above. The retention of the drug in the prepared liposomes was calculated by dividing the drug to phospholipid ratio at indicated time point by the initial drug to phospholipid ratio.

2.5. Partitioning of l-OHP into erythrocytes

Either free l-OHP solution or l-OHP encapsulated in PEG-coated cationic liposomes was injected intravenously in mice. Blood was collected at 3 and 6 h post injection in the presence of anticoagulant (heparin) and centrifuged to obtain plasma and the precipitate containing erythrocytes (erythrocytes fraction). l-OHP in plasma and erythrocytes was determined as described above. The percent of l-OHP partitioning in plasma and erythrocytes at each time point was calculated using the following formula:

$$\%\text{1-OHP partitioning} = \frac{\%\,\text{dose of 1-OHP in plasma or erythrocytes}}{\%\,\text{dose of 1-OHP in whole blood}}$$

2.6. Mouse dorsal air sac (DAS) model

The mouse DAS model was developed according to the method described by Nakamura et al. [29,30] with minor modification. Briefly,

Table 1
In vitro retention of l-OHP in PEG-coated cationic liposomes or PEG-coated neutral liposomes

Formulation		Retention of l-OHP (%)			
		1 h	3 h	6 h	24 h
PEG-coated cationic liposomes	50% Plasma	89.10	81.54	73.09	61.86
	5% Dextrose	99.70	94.50	88.90	85.16
PEG-coated neutral liposomes	50% Plasma	92.55	84.01	77.47	64.72
	5% Dextrose	97.82	97.80	89.45	83.63

Retention of l-OHP was determined at different times during incubation with the formulation in either 50% plasma or 5% dextrose at 37 °C.

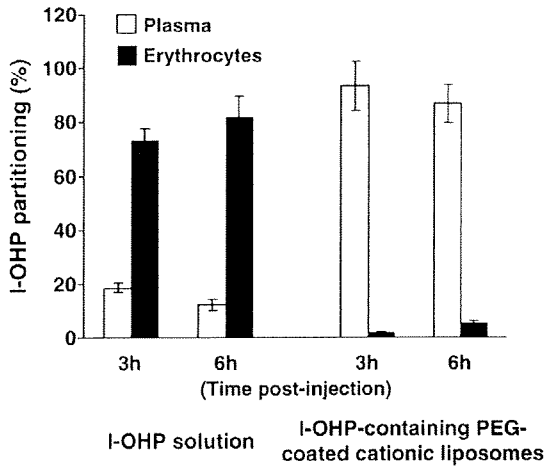

Fig. 1. Partitioning of I-OHP encapsulated in PEG-coated cationic liposomes into erythrocytes. Mice received intravenous injection with either free I-OHP solution or I-OHP-containing PEG-coated cationic liposomes. After 3 or 6 h injection, blood was collected, and the amount of I-OHP in plasma and erythrocytes was determined. Data are presented as the percentage of I-OHP partitioning in injected I-OHP dose. Data represents the mean±S.D. (n=3).

a chamber, which was prepared by covering both sides of a Millipore ring (10 mm diameter, 3 mm thickness) with Millipore filters (0.45-μm pore size), was filled with a suspension of B16BL6 tumor cells (1×10^7 cells) in 0.18 ml of DMEM. The chamber was then implanted into the subcutaneous dorsal air sac created by subcutaneous injection of 10 ml of air in anesthetized (25 mg/kg pentobarbital, i.p.) male ddY mice. At different days after chamber implantation, the animals were sacrificed and the skin was removed. The implanted chambers were removed from the subcutaneous fascia of the animals, and a black ring with the same inner diameter as that of the Millipore ring was placed at the same site. The angiogenic response, indicated by the formation of zigzag-shaped blood vessels, was observed under dissecting microscope (STeREO Lumar. V12, Zeiss, Germany).

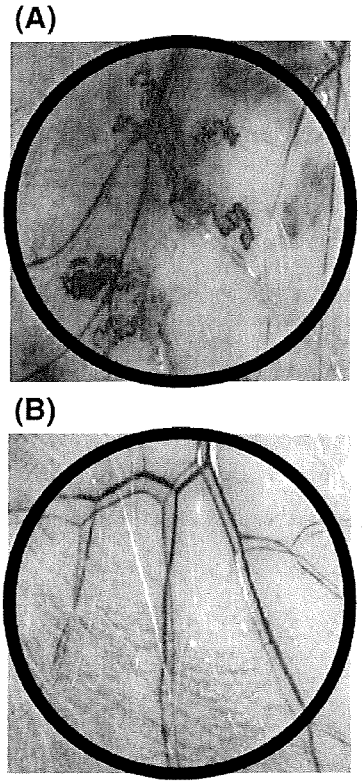

Fig. 2. Angiogenesis in the mouse DAS model. (A) Photograph of skin area attached to a chamber containing tumor cells (positive control). (B) Photograph of skin area attached to a chamber containing only DMEM (no tumor cells, negative control). 8x magnification.

2.7. Intracutaneous distribution of DiI-labeled liposomes

To induce neo-vascularization, a chamber containing tumor cells was implanted in the dorsal skin of the mouse. Five days later, DiI-labeled liposomes (no I-OHP, 45 mg total lipid/ mice) were intravenously administered. Eight hours later, the animal was sacrificed, and then the back-skin was removed. The area attached to the chamber was observed under the fluorescence microscope (STeREO Lumar. V12, Zeiss, Germany) to detect the accumulation of the liposomes in the newly formed vessels.

2.8. Evaluation of the anti-angiogenic effect of various I-OHP formulations

The *in vivo* anti-angiogenic activity of different I-OHP formulations was evaluated by using the DAS assay as follows.

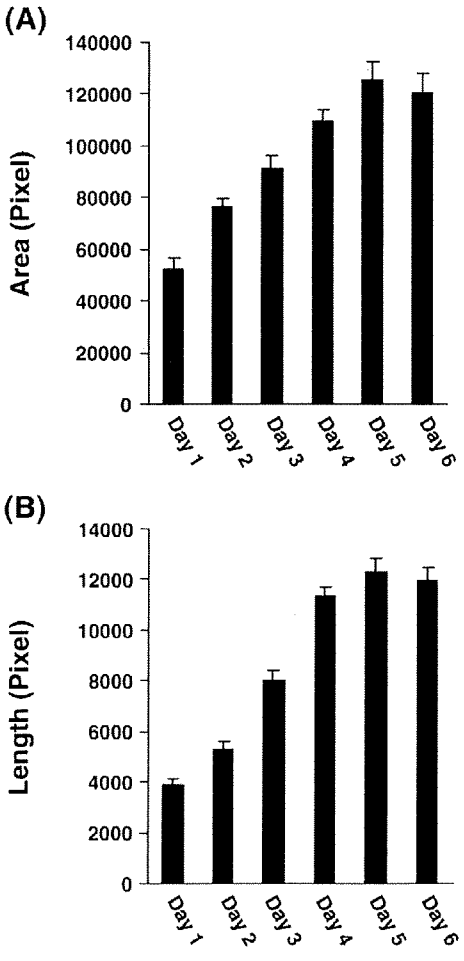

Fig. 3. Characterization of the mouse DAS model. Tumor-induced angiogenesis was evaluated sequentially from day 1 to day 6 post-chamber implantation. (A) represents the capillary network area of newly formed vessels. (B) represents the length of newly formed vessels. The values represent the mean±S.D. (n=3).

Experiment 1: Mice carrying the implanted chambers were treated with an intravenous injection of l-OHP encapsulated in PEG-coated cationic liposomes (5 mg l-OHP/kg, 45 mg total lipid/mouse) once on day 1, 2, 3 or 4 after chamber implantation. Mice carrying an implanted chamber and receiving no l-OHP treatment served as positive controls. Mice carrying an implanted chamber containing DMEM instead of tumor cells and receiving no l-OHP treatment served as negative controls. On day 5 after chamber implantation, angiogenesis was assessed by determining the dense capillary network area and length of angiogenic vessels in the area attached to the chamber using an Angiogenesis Image Analyzer (version 2, Kurabo).

Experiment 2: Mice (n=20) carrying implanted chambers containing tumor cells were divided into four groups. The first group received l-OHP-containing PEG-coated cationic liposomes (5 mg l-OHP/kg, 45 mg total lipid/mouse). The second group received "empty" (no drug) PEG-coated cationic liposomes (45 mg total lipid/mouse). The third group received l-OHP-containing PEG-coated neutral liposomes (5 mg l-OHP/kg). The last group received l-OHP solution (5 mg l-OHP/kg). All groups received the treatment via tail vein on the third day after chamber implantation. The angiogenesis was assessed as described above.

2.9. Statistical analysis

All values were expressed as the mean ± S.D. Statistical analysis was performed with the analysis of variance (ANOVA) test using GraphPad software (GraphPad Software, CA, USA). The level of significance was set at $p<0.05$.

3. Results

3.1. Characterization of liposomes

The size and zeta potential of l-OHP-containing liposomes were determined. The size of PEG-coated cationic liposomes was 250±10 nm and the zeta potential was 11.24±0.7 mV. The size of PEG-coated neutral liposomes (control liposomes) was 245±6 nm and the zeta potential −6.9±0.9 mV. The encapsulation efficiency of l-OHP was 25.4% for PEG-coated cationic liposomes and 22.0% for PEG-coated neutral liposomes.

Following storage in 5% dextrose at 4 °C for 4 weeks, the particle size of both formulations was changed slightly; 257±17 nm for PEG-coated cationic liposomes and 249±15 nm for PEG-coated neutral liposomes. This suggests that both formulations were stable in terms of size distribution during storage at 4 °C at least for 4 weeks.

3.2. In vitro stability of l-OHP liposomal formulations

We examined the retention of l-OHP in the liposomes upon incubation in 5% dextrose at 4 °C for up to 1 week. More than 80% of the encapsulated l-OHP still remained inside PEG-coated cationic liposomes and PEG-coated neutral liposomes (not shown). Then, the retention of the encapsulated l-OHP was investigated upon incubation in either 5% dextrose or 50% mouse plasma at 37 °C. As shown in Table 1, no remarkable difference was observed on the l-OHP retention between both liposomes, although 35–40% of encapsulated l-OHP was released following 24 h incubation. Moreover, it was shown that mouse plasma enhanced release rate of l-OHP from the liposomes, as

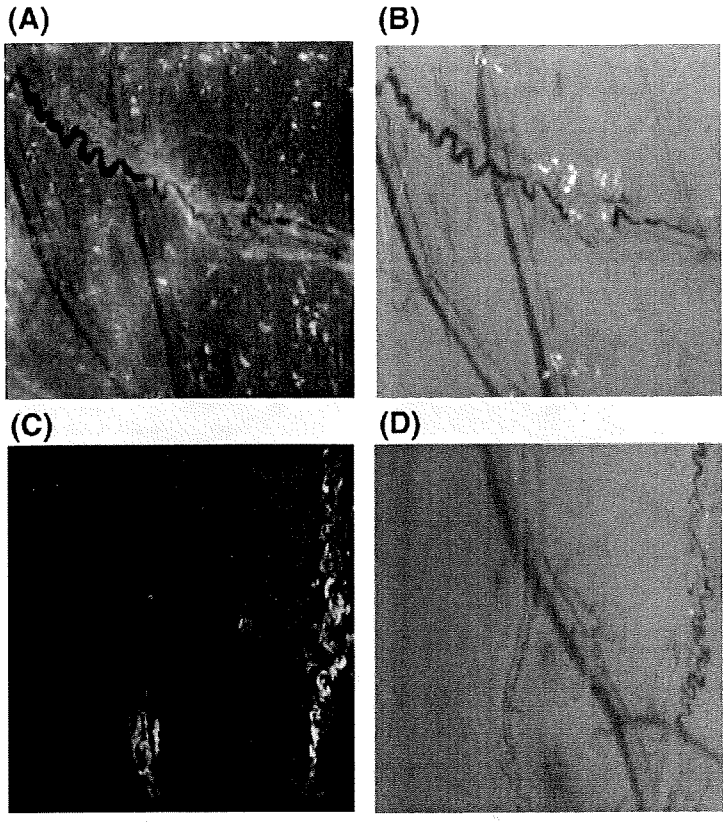

Fig. 4. Selectivity of PEG-coated cationic liposomes to newly formed blood vessels in the DAS model. (A) Skin area attached to a chamber 8 h after intravenous administration of DiI-labeled PEG-coated neutral liposomes observed by fluorescence microscopy. (B) Same area as in (A) under normal light. (C) Skin area attached to a chamber 8 h after intravenous administration of DiI-labeled PEG-coated cationic liposomes as seen by fluorescence microscopy. (D) Same area as in (C) under normal light. Each photograph is a representative example of at least 5 replicate experiments. 20x magnification.

compared with 5% dextrose. It appears that plasma proteins induce the leakage of l-OHP from both liposomes.

3.3. Partitioning of liposomal l-OHP into erythrocytes

The extent of partitioning of either free l-OHP or l-OHP encapsulated in PEG-coated cationic liposomes into erythrocytes was investigated at 3 and 6 h after intravenous injection of either free l-OHP solution or l-OHP encapsulated in PEG-coated cationic liposome. As l-OHP solution was injected, l-OHP was extensively taken up by erythrocytes (73.05% and 81.95% dose at 3-hour- and 6-hour post injection, respectively) and a small free fraction was available in plasma (Fig. 1). On the other hand, for l-OHP encapsulated in PEG-coated cationic liposomes, more than 90% dose of l-OHP was detected in plasma at each time point, while a little l-OHP (less than 10% dose) was taken up by erythrocytes (Fig. 1). These observations suggest that l-OHP-containing PEG-coated cationic liposomes were stable in blood circulation.

3.4. Characterization of DAS model

We first determined whether the DAS model induces *in vivo* angiogenesis. Newly formed microvessels having a zigzag-shape were abundantly produced as a result of the implantation of the tumor cells-containing chamber (Fig. 2A). Upon the implantation of chambers containing no tumor cells (negative controls) minimal angiogenesis was induced (Fig. 2B). This indicates that tumor cells, not the experimental manipulation and subsequent healing process, evoke a significant angiogenic response.

We then determined the optimal day for evaluating the angiogenic response induced by implantation of the tumor cells-containing chamber. As shown in Fig. 3A and B, the angiogenic response, as indicated by the dense capillary network area and length of angiogenic vessels, increased day by day and reached a maximum level on the fifth day post-chamber implantation. We therefore decided day 5 post-chamber implantation as a standard time point for evaluating angiogenesis in all subsequent experiments.

3.5. Selectivity of PEG-coated cationic liposome targeting to angiogenic blood vessels in the DAS model

The selectivity of PEG-coated cationic liposomes for the newly formed vessels was investigated in the DAS model. Eight hours after intravenous injection, control liposomes (PEG-coated neutral liposomes) had extravasated extensively into the interstitium in the skin, presumably through the leaky vasculature (Fig. 4A and B). By contrast, the PEG-coated cationic liposomes showed avid association with the newly formed vessels without any extravasation into the skin interstitium (Fig. 4C and D). No such accumulation of cationic liposomes was observed in the skin area attached to chambers containing only DMEM (data not shown). These observations indicate that the cationic liposomes possess selectivity to angiogenic vessels.

3.6. In vivo anti-angiogenic effect of l-OHP-containing PEG-coated cationic liposomes

The *in vivo* anti-angiogenic activity of l-OHP-containing PEG-coated cationic liposomes was investigated in the DAS assay. The l-OHP preparation was intravenously administered on day 1, 2, 3 or 4 after chamber implantation and the effect on neo-vascularization was examined microscopically on day 5. The photographs demonstrate that injection of cationic liposomes containing l-OHP on day 1 or 2 did

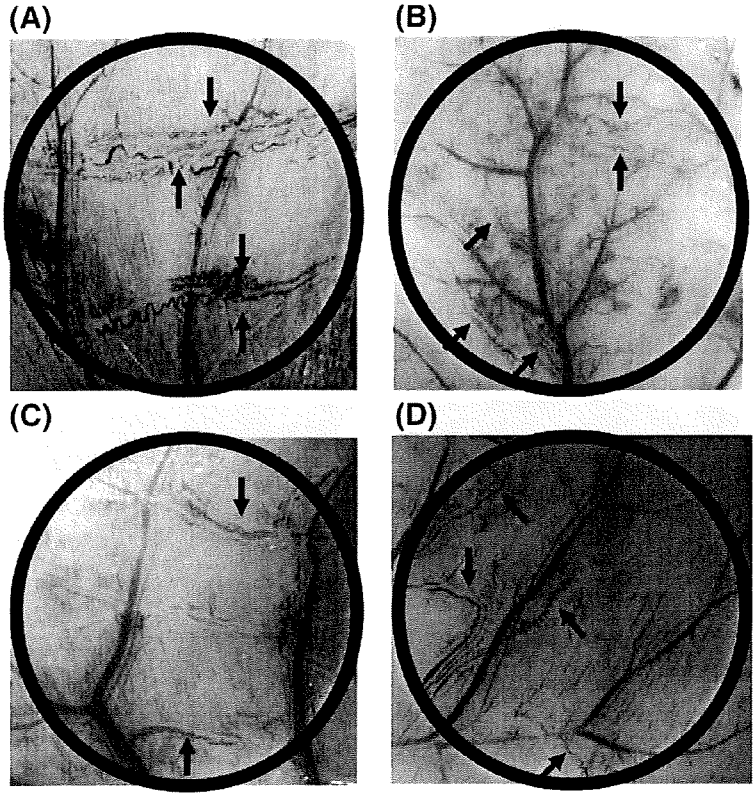

Fig. 5. Optical observation of the *in vivo* anti-angiogenic effect of l-OHP-containing PEG-coated cationic liposomes. Mice with an implanted chamber received l-OHP-containing PEG-coated cationic liposomes (5 mg l-OHP/kg) via tail vein on day 1 (A), 2 (B), 3 (C) or 4 (D) after chamber implantation. On day 5, the area of skin attached to the chamber was microscopically examined. Each photograph is a representative example of at least 5 replicate experiments. Arrow heads represent newly formed vessels. 8x magnification.

not suppress the angiogenesis (Fig. 5A and B), relative to the control group (Fig. 2A), while injection on day 3 or 4 strongly suppressed angiogenesis (Fig. 5C and D). A quantitative evaluation of the anti-angiogenic effect was obtained by determining the capillary network area and length of angiogenic vessels on the micrographs. Significant suppression of angiogenesis in terms of both area and length of vessels was observed in all treated groups when compared with the positive control (ANOVA, $p<0.05$) (Fig. 6A and B). Notably, the treatment on day 3 completely suppressed the angiogenesis to the negative control level. The results clearly indicate that l-OHP encapsulated in liposomes which are targeted to newly forming vessels can suppress angiogenesis with an efficacy that appears to depend on the time of administration.

3.7. Specificity of in vivo anti-angiogenic effect of l-OHP-containing PEG-coated cationic liposomes

On day 3 after chamber implantation, the efficacy of the *in vivo* anti-angiogenic effect of l-OHP-containing PEG-coated cationic liposomes was compared with that of free l-OHP, l-OHP-containing PEG-coated neutral liposomes and "empty" (no drug-containing) PEG-coated cationic liposomes (Fig. 7A and B). Free l-OHP and empty PEG-coated cationic liposomes caused only a slight suppression of angiogenesis. PEG-coated neutral liposomes induced a stronger suppression of angiogenesis than free l-OHP and empty PEG-coated cationic liposomes. PEG-coated cationic liposomes resulted in efficient anti-angiogenic activity superior to all other l-OHP formulations (ANOVA, $p<0.05$).

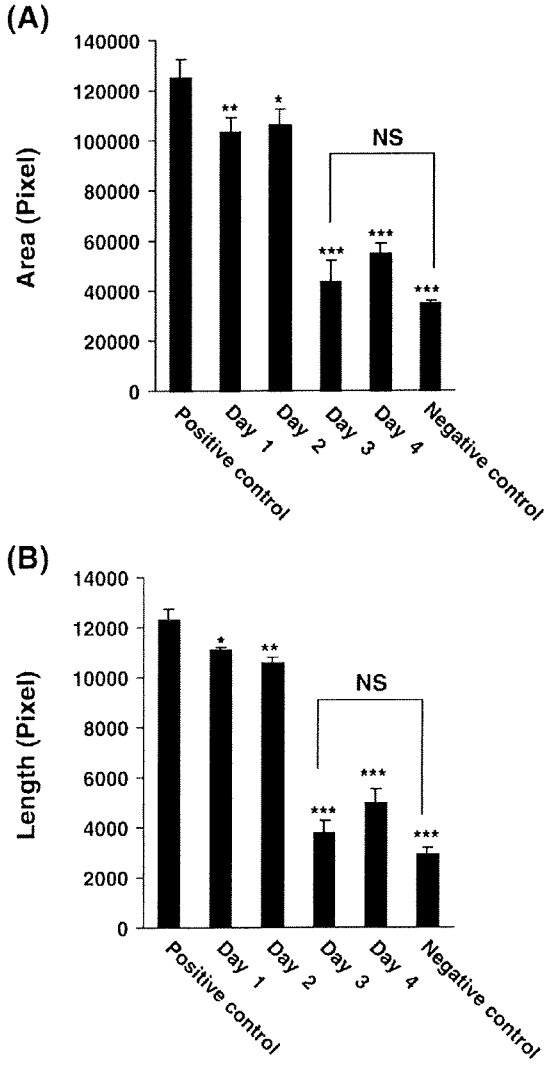

Fig. 6. Quantification of *in vivo* anti-angiogenic effect of l-OHP-containing PEG-coated cationic liposomes. The capillary network area (A) and length of newly formed vessels (B) in the area of skin attached to the chamber were measured on the basis of the photographs presented in Fig. 5. The values (n=5) represent the mean±S.D. * $p<0.05$, ** $p<0.01$, *** $p<0.005$ vs positive control; NS, not significantly different from the values at day 3 and negative control.

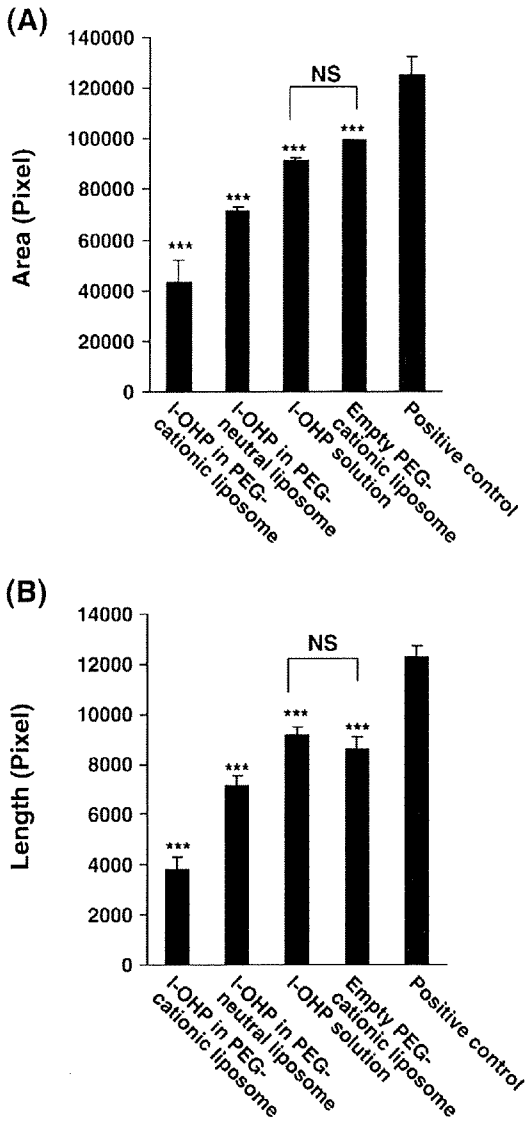

Fig. 7. Specificity of the in vivo anti-angiogenic effect of l-OHP-containing PEG-coated cationic liposomes. The anti-angiogenic effect of l-OHP-containing PEG-coated cationic liposome was compared with that of other formulations, i.e. free l-OHP, l-OHP encapsulated in PEG-coated neutral liposomes and "empty" (no drug containing) PEG-coated cationic liposomes. Mice with an implanted chamber received the formulations (5 mg l-OHP/kg, 45 mg total lipid/mouse) on day 3 after chamber implantation. On day 5, the skin area attached to the chamber was examined microscopically. The capillary network area (A) and length of newly formed vessels (B) on photographs taken were quantitatively determined. The values (n=5) represent the mean±S.D. The data for l-OHP-containing PEG-coated cationic liposomes and positive control were taken from the Fig. 6. *** $p<0.005$ vs positive control; NS, not significant.

4. Discussion

The purpose of this study was to develop a selective delivery system for l-OHP to areas of tumor-induced angiogenesis and to evaluate the

anti-angiogenic efficacy of l-OHP using the *in vivo* mouse DAS model. We chose for the use of cationic liposomes, because these have been reported to display a strong binding ability to tumor-derived angiogenic vascular endothelial cells due to the strong electrostatic adhesion between the cationic surface and the plasma membrane [32,33]. We modified the surface of cationic liposomes with $mPEG_{2000}$-DSPE, which makes it possible to prolong the circulation time of the liposomes by preventing interactions with the biological *in vivo* environment [34] thus enhancing their chance to gain access to the target angiogenic vessels. Our results indicate that the PEG-coated cationic liposomes we designed exhibit a selective accumulation/binding to the newly formed vessels (Fig. 4). In addition, no selective accumulation/binding of the liposomes to pre-existing blood vessels in the skin was observed (Fig. 4C and D). This points to an important difference in distribution of liposomes in blood vessels between normal tissues and tumor tissue, which may be exploited while attempting to achieve successful anti-angiogenic chemotherapy.

So far, free l-OHP has not been reported to suppress tumor-related angiogenesis, a crucial event in solid tumor growth [35,36]. This can probably be attributed to a low anti-tumor activity of l-OHP as a result of its high partitioning to erythrocytes and low accumulation in tumor tissues [6,7]. In the present study, a single injection of l-OHP encapsulated in PEG-coated cationic liposomes achieved complete suppression of angiogenesis in the DAS assay, while injection of either free l-OHP or l-OHP encapsulated in PEG-coated neutral liposomes only very slightly suppressed angiogenesis (Fig. 7). To the best of our knowledge, this is the first published observation of an anti-angiogenic effect of l-OHP. We assume that as a consequence of the selective delivery of l-OHP to the angiogenic vessels and its subsequent uptake by endothelial cells [13] the local concentration of the drug in/around proliferative vascular endothelial cells is increased. By contrast, the other l-OHP formulations are likely to suffer from high partitioning to erythrocytes (especially free l-OHP formulation) or massive distribution to the skin interstitium (especially PEG-coated neutral liposome formulation) (Fig. 4A), leading to an insufficiently high local drug concentration to exert a therapeutic effect.

In view of the results demonstrated in Figs. 5 and 6, it seems that the anti-angiogenic effect of l-OHP encapsulated in PEG-coated cationic liposomes is dependent on the time of drug administration. During the first 2 days after chamber implantation when the process of angiogenesis is not yet fully activated, the area to which the targeted liposomes can bind and thus site of action of the drug will be rather insignificant. At day 3 or 4 after the chamber implantation, however, when proliferation of endothelial cells is maximally activated, both the binding area of the liposomes and the site of action of the drug will be much larger. This is likely to be highly relevant to the clinical situation in case of tumor growth in that the efficacy of our l-OHP formulation is thought to depend on tumor progression which, in turn, strongly related to angiogenic-microvessel density.

Among various widely accepted methods used to evaluate the inhibition of angiogenesis [37], we selected the DAS model [29,30], a common and a reliable method, to evaluate the selectivity of PEG-coated cationic liposomes and the anti-angiogenic effects of liposome-encapsulated l-OHP. The DAS model is technically simple, provides a natural environment in which blood vessels and their tumor-induced formation can be studied. In addition, the model takes only about 5 days to develop and is therefore less time-consuming than the tumor-bearing mouse model, which takes more than 10 days. Therefore, the DAS model is a convenient and reliable method to effectively screen nanomolecular drug delivery systems targeting to tumor-induced neo-vascularization and evaluate the anti-angiogenic efficacy of the drug delivery system.

In recent years, l-OHP-based chemotherapy protocols, particularly l-OHP in combination with the infusion of 5-fluorouracil/leucovorin (FOLFOX), have emerged as the standard care in first- and second-line therapy of advanced-stage colorectal cancer [38,39]. In contrast to cisplatin, l-OHP has no renal toxicity, only mild hematological and gastrointestinal toxicity, while neurotoxicity is the dose-limiting toxicity [40,41]. This side effect has been described as a transient distal dysesthesia, enhanced by exposure to cold, and as a dose-related cumulative mild sensitive neuropathy [40,41]. The selective delivery of l-OHP to newly formed tumor-induced blood vessels as described here or to tumor tissues [6] by nanomolecular drug delivery systems raises the possibility of reducing the total l-OHP dose for the dosing regimen such as FOLFOX. This would improve the tolerance of patients and thereby improve the therapeutic efficacy as compared to the standard treatment protocols. Thus, the in vivo anti-angiogenic effect of our l-OHP formulation may lead to significant improvements in terms of survival rates and quality of life of patients with colorectal cancer.

Acknowledgments

We thank Dr. G.L. Scherphof for his helpful advice in preparing this manuscript. This study was supported, in part, by the Kobayashi Fund for Cancer Research and the Knowledge Cluster Initiative from Ministry of Education, Science and Technology.

References

[1] T. Nishikawa, N. Akiyama, K. Kunimasa, T. Oikawa, M. Ishizuka, M. Tsujimoto, S. Natori, Inhibition of in vivo angiogenesis by N-beta-alanyl-5-S-glutathionyl-3,4 dihydroxyphenylalanine, Eur. J. Pharmacol. 539 (2006) 151–157.
[2] T. Masuda, S. Ohba, M. Kawada, M. Osono, D. Ikeda, H. Esumi, S. Kunimoto, Antitumor effect of kigamicin D on mouse tumor models, J. Antibiot. (Tokyo) 59 (2006) 209–214.
[3] Y. Basaki, L. Chikahisa, K. Aoyagi, K. Miyadera, K. Yonekura, A. Hashimoto, S. Okabe, K. Wierzba, Y. Yamada, Gamma-hydroxybutyric acid and 5-fluorouracil, metabolites of UFT, inhibit the angiogenesis induced by vascular endothelial growth factor, Angiogenesis 4 (2001) 163–173.
[4] T. Tashiro, Y. Kawada, Y. Sakurai, Y. Kidani, Antitumor activity of a new platinum complex, oxalato (trans-l-1,2-diaminocyclohexane)platinum (II): new experimental data, Biomed. Pharmacother. 43 (1989) 251–260.
[5] K. Yonekura, Y. Basaki, L. Chikahisa, S. Okabe, A. Hashimoto, K. Miyadera, K. Wierzba, Y. Yamada, UFT and its metabolites inhibit the angiogenesis induced by murine renal cell carcinoma, as determined by a dorsal air sac assay in mice, Clin. Cancer Res. 5 (1999) 2185–2191.
[6] R. Suzuki, T. Takizawa, Y. Kuwata, M. Mutoh, N. Ishiguro, N. Utoguchi, A. Shinohara, M. Eriguchi, H. Yanagie, K. Maruyama, Effective anti-tumor activity of oxaliplatin encapsulated in transferrin-PEG-liposome, Int. J. Pharm. 346 (2008) 143–150.
[7] L. Pendyala, P.J. Creaven, In vitro cytotoxicity, protein binding, red blood cell partitioning, and biotransformation of oxaliplatin, Cancer Res. 53 (1993) 5970–5976.
[8] Y. Yu, L.G. Lou, W.P. Liu, H.J. Zhu, Q.S. Ye, X.Z. Chen, W.G. Gao, S.Q. Hou, Synthesis and anticancer activity of lipophilic platinum(II) complexes of 3,5-diisopropylsalicylate, Eur. J. Med. Chem. (2007).
[9] R.D. Hofheinz, S.U. Gnad-Vogt, U. Beyer, A. Hochhaus, Liposomal encapsulated anti-cancer drugs, Anticancer Drugs 16 (2005) 691–707.
[10] A.Z. Dudek, W.Z. Pawlak, M.N. Kirstein, Molecular targets in the inhibition of angiogenesis, Expert Opin. Ther. Targets 7 (2003) 527–541.
[11] K. Shimizu, N. Oku, Cancer anti-angiogenic therapy, Biol. Pharm. Bull 27 (2004) 599–605.
[12] J. Ye, Y. Li, T. Hamasaki, N. Nakamichi, T. Komatsu, T. Kashiwagi, K. Teruya, R. Nishikawa, T. Kawahara, K. Osada, K. Toh, M. Abe, H. Tian, S. Kabayama, K. Otsubo, S. Morisawa, Y. Katakura, S. Shirahata, Inhibitory effect of electrolyzed reduced water on tumor angiogenesis, Biol. Pharm. Bull. 31 (2008) 19–26.
[13] G. Thurston, J.W. McLean, M. Rizen, P. Baluk, A. Haskell, T.J. Murphy, D. Hanahan, D.M. McDonald, Cationic liposomes target angiogenic endothelial cells in tumors and chronic inflammation in mice, J. Clin. Invest. 101 (1998) 1401–1413.
[14] R.S. Kerbel, Tumor angiogenesis: past, present and the near future, Carcinogenesis 21 (2000) 505–515.
[15] N.M. Pandya, N.S. Dhalla, D.D. Santani, Angiogenesis—a new target for future therapy, Vasc. Pharmacol. 44 (2006) 265–274.
[16] T. Asahara, T. Takahashi, H. Masuda, C. Kalka, D. Chen, H. Iwaguro, Y. Inai, M. Silver, J.M. Isner, VEGF contributes to postnatal neovascularization by mobilizing bone marrow-derived endothelial progenitor cells, Embo J. 18 (1999) 3964–3972.
[17] D. Lyden, K. Hattori, S. Dias, C. Costa, P. Blaikie, L. Butros, A. Chadburn, B. Heissig, W. Marks, L. Witte, Y. Wu, D. Hicklin, Z. Zhu, N.R. Hackett, R.G. Crystal, M.A. Moore, K.A. Hajjar, K. Manova, R. Benezra, S. Rafii, Impaired recruitment of bone-marrow-derived endothelial and hematopoietic precursor cells blocks tumor angiogenesis and growth, Nat. Med. 7 (2001) 1194–1201.
[18] C.A. Staton, S.M. Stribbling, S. Tazzyman, R. Hughes, N.J. Brown, C.E. Lewis, Current methods for assaying angiogenesis in vitro and in vivo, Int. J. Exp. Pathol. 85 (2004) 233–248.

[19] S. Hussain, M. Slevin, S. Matou, N. Ahmed, M.I. Choudhary, R. Ranjit, D. West, J. Gaffney, Anti-angiogenic activity of sesterterpenes: natural product inhibitors of FGF-2-induced angiogenesis, Angiogenesis 11 (2008) 245–256.
[20] R. Kumar, J. Yoneda, C.D. Bucana, I.J. Fidler, Regulation of distinct steps of angiogenesis by different angiogenic molecules, Int. J. Oncol. 12 (1998) 749–757.
[21] T. Shibusa, N. Shijubo, S. Abe, Tumor angiogenesis and vascular endothelial growth factor expression in stage I lung adenocarcinoma, Clin. Cancer Res. 4 (1998) 1483–1487.
[22] L.S. Rosen, Clinical experience with angiogenesis signaling inhibitors: focus on vascular endothelial growth factor (VEGF) blockers, Cancer Control 9 (2002) 36–44.
[23] J. Folkman, The role of angiogenesis in tumor growth, Semin. Cancer Biol. 3 (1992) 65–71.
[24] M. Asano, A. Yukita, T. Matsumoto, S. Kondo, H. Suzuki, Inhibition of tumor growth and metastasis by an immunoneutralizing monoclonal antibody to human vascular endothelial growth factor/vascular permeability factor121, Cancer Res. 55 (1995) 5296–5301.
[25] B. Millauer, M.P. Longhi, K.H. Plate, L.K. Shawver, W. Risau, A. Ullrich, L.M. Strawn, Dominant-negative inhibition of Flk-1 suppresses the growth of many tumor types in vivo, Cancer Res. 56 (1996) 1615–1620.
[26] R.B. Campbell, D. Fukumura, E.B. Brown, L.M. Mazzola, Y. Izumi, R.K. Jain, V.P. Torchilin, L.L. Munn, Cationic charge determines the distribution of liposomes between the vascular and extravascular compartments of tumors, Cancer Res. 62 (2002) 6831–6836.
[27] S. Strieth, M.E. Eichhorn, B. Sauer, B. Schulze, M. Teifel, U. Michaelis, M. Dellian, Neovascular targeting chemotherapy: encapsulation of paclitaxel in cationic liposomes impairs functional tumor microvasculature, Int. J. Cancer 110 (2004) 117–124.
[28] A.V. Kalra, R.B. Campbell, Development of 5-FU and doxorubicin-loaded cationic liposomes against human pancreatic cancer: implications for tumor vascular targeting, Pharm. Res. 23 (2006) 2809–2817.
[29] M. Nakamura, Y. Katsuki, Y. Shibutani, T. Oikawa, Dienogest, a synthetic steroid, suppresses both embryonic and tumor-cell-induced angiogenesis, Eur. J. Pharmacol. 386 (1999) 33–40.
[30] T. Oikawa, M. Sasaki, M. Inose, M. Shimamura, H. Kuboki, S. Hirano, H. Kumagai, M. Ishizuka, T. Takeuchi, Effects of cytogenin, a novel microbial product, on embryonic and tumor cell-induced angiogenic responses in vivo, Anticancer Res. 17 (1997) 1881–1886.
[31] G.R. Bartlett, Colorimetric assay methods for free and phosphorylated glyceric acids, J. Biol. Chem. 234 (1959) 469–471.
[32] T. Nomura, N. Koreeda, F. Yamashita, Y. Takakura, M. Hashida, Effect of particle size and charge on the disposition of lipid carriers after intratumoral injection into tissue-isolated tumors, Pharm. Res. 15 (1998) 128–132.
[33] Y. Takeuchi, K. Kurohane, K. Ichikawa, S. Yonezawa, M. Nango, N. Oku, Induction of intensive tumor suppression by antiangiogenic photodynamic therapy using polycation-modified liposomal photosensitizer, Cancer 97 (2003) 2027–2034.
[34] C. Allen, N. Dos Santos, R. Gallagher, G.N. Chiu, Y. Shu, W.M. Li, S.A. Johnstone, A.S. Janoff, L.D. Mayer, M.S. Webb, M.B. Bally, Controlling the physical behavior and biological performance of liposome formulations through use of surface grafted poly(ethylene glycol), Biosci. Rep. 22 (2002) 225–250.
[35] C.J. Gomer, Preclinical examination of first and second generation photosensitizers used in photodynamic therapy, Photochem. Photobiol. 54 (1991) 1093–1107.
[36] B.W. Henderson, T.J. Dougherty, How does photodynamic therapy work? Photochem. Photobiol. 55 (1992) 145–157.
[37] R.K. Jain, K. Schlenger, M. Hockel, F. Yuan, Quantitative angiogenesis assays: progress and problems, Nat. Med. 3 (1997) 1203–1208.
[38] A. de Gramont, A. Figer, M. Seymour, M. Homerin, A. Hmissi, J. Cassidy, C. Boni, H. Cortes-Funes, A. Cervantes, G. Freyer, D. Papamichael, N. Le Bail, C. Louvet, D. Hendler, F. de Braud, C. Wilson, F. Morvan, A. Bonetti, Leucovorin and fluorouracil with or without oxaliplatin as first-line treatment in advanced colorectal cancer, J. Clin. Oncol. 18 (2000) 2938–2947.
[39] C. Tournigand, T. Andre, E. Achille, G. Lledo, M. Flesh, D. Mery-Mignard, E. Quinaux, C. Couteau, M. Buyse, G. Ganem, B. Landi, P. Colin, C. Louvet, A. de Gramont, FOLFIRI followed by FOLFOX6 or the reverse sequence in advanced colorectal cancer: a randomized GERCOR study, J. Clin. Oncol. 22 (2004) 229–237.
[40] A. Grothey, Oxaliplatin-safety profile: neurotoxicity, Semin. Oncol. 30 (2003) 5–13.
[41] A. Pietrangeli, M. Leandri, E. Terzoli, B. Jandolo, C. Garufi, Persistence of high-dose oxaliplatin-induced neuropathy at long-term follow-up, Eur. Neurol. 56 (2006) 13–16.